Environmental Science and Pollution Research
https://doi.org/10.1007/s11356-020-10818-9

RESEARCH ARTICLE

Sources and selective preservation of organic matter in the karst watershed: evidence from sediment records in a plateau deep lake, Southwestern China

Runyu Zhang [1] · Liying Wang [1] · Jingan Chen [1]

Received: 7 May 2020 / Accepted: 10 September 2020

Abstract

Human activities have greatly altered terrestrial carbon (C) dynamics associated with vegetation cover and land use changes, thereby influencing the C sink in downstream ecosystems. However, the transport and preservation of organic C from soils that experience serious erosion in the karst area are scarce, particularly at catchment scales. In this study, chemical characteristics of organic matter (OM) isolated from the topsoil, overlying water, and lake sediments, as well as subsequent source identification, were inferred from the molecular, spectroscopic, and carbon isotopic ($\delta^{13}C$) signatures in a typical karst catchment, Southwestern China. The results indicated that the elemental compositions of the calcareous soil and paddy soil significantly differed from the yellow soil. High similarities existed in the fluorescence spectra of humic substances (HS) extracted from the front two soil types with those of lake sediments, indicating the homogeneous nature of OM molecular structure. The C/N ratios of six dissolved OM fractions and sedimentary HS along with $\delta^{13}C$ values consistently reflected the primary terrestrial source. It was estimated to account for 60% of total organic C in sedimentary OM by end-member mixing modeling in accordance with soil erosion intensity and large recharge coefficient of this catchment. The evolution of soil loss and lake productivity can be well deduced from sediment records of organic C content, C/N ratio, and the specific information of HS. This research highlighted that the composition, source, and fate of OM in the karst lake was mainly dominated by the terrestrial C flux, rather than in-lake production. Furthermore, soil type and erosion intensity have significant effects on the nature of eroded OM and ultimate preservation.

Keywords Karst watershed · Soil erosion · Carbon sink · Humic substances · Sediment record

Introduction

Karst topography is one of the most fragile and vulnerable environments because of the low pedogenesis and high permeability underlying the carbonate rocks (Jiang et al. 2014). It represents 7–12% of the global land surface and is widely distributed in the Mediterranean coast, Southwest China, Northern Vietnam, Indiana and Kentucky of the USA, Cuba, and Jamaica (Li et al. 2016). As one of the three largest continuous and well-developed karst landforms in the world, Southwest China amounted to 2.5% of the global karst area, about 540 000 km^2 (Luo et al. 2016). Over the past several centuries, excessive deforestation and reclaiming of lands for cultivation have resulted in considerable land depression and soil erosion here, thereby threatening the livelihoods of more than 200 million residents (Jiang and Ji 2013; Luo et al. 2016). Moreover, lateral movement of sediment and water in the soil system transports a great amount of the terrestrial C to downstream water bodies such as river and lakes via runoff, leaching, and subsurface flow processes (Wang et al. 2008; Li et al. 2016; Lu et al. 2018).

Nowadays, inland lake is increasingly recognized as playing an important role in the transport, mineralization, and burial of terrestrial C, especially in the karst watershed (Nõges et al. 2016; Sironić et al. 2017; Lu et al. 2018). It has been estimated that 2.9 Pg C a^{-1} discharged from global landscapes, in which about 20 percent was detained in the

Responsible editor: Kitae Baek

✉ Runyu Zhang
zhangrunyu@vip.gyig.ac.cn

[1] State Key Laboratory of Environmental Geochemistry, Institute of Geochemistry, Chinese Academy of Sciences, Guiyang 550081, China

Published online: 19 September 2020

freshwater sediments (Cole et al. 2007; Tranvik et al. 2009). Among them, approximately 11–46% of organic C inputs were permanently captured by lakes, which originated from allochthonous or/and autochthonous organic matter (OM) (Sobek et al. 2009; Lu et al. 2018). Human activities can largely affect the origin, transport, and fate of organic C in the lake ecosystem (Li et al. 2016; Nõges et al. 2016). Recent studies have shown that the burial rate of organic C rose dramatically in the subtropical lakes of Southwest China in the past decades in response to increasing agricultural intensification and urban expansion (Wang et al. 2018; He et al. 2020). However, the patterns of the lake C enrichment and the depositional processes in the karst watershed differed from those of other geologic settings because of the distinct hydrological processes of runoff, sediment yield, and nutrient transportation (Jiang and Ji 2013; Li et al. 2016). Little information is currently available on the composition and transformation mechanism of OM, especially organic C, as it moves through karst ecosystems (Nõges et al. 2016; Lechleitner et al. 2017).

Lake sediments are valuable archives of paleoenvironmental change by way of containing a diverse range in the catchment and/or in the water body. The elemental composition of sedimentary OM can be used as an effective fingerprint to better inform regional environment succession (Jiang and Ji 2013; Luo et al. 2019). Currently, C/N ratios along with multiple isotopic signatures (e.g., $\delta^{13}C$, $\delta^{15}N$) of particulate or sedimentary OM are regarded as customary indicators to discriminate the sources of OM and reconstruct past environment change (Meyers and Ishiwatari 1993; Jiang and Ji 2013; Luo et al. 2019). However, these methods are difficult to accurately discern the differences between endogenous and exogenous OM and quantified their respective proportions based on global statistics rather than a specific region (Perdue and Koprivnjak, 2007; Jiang and Ji 2013). Furthermore, both proxies are susceptible to diagenetic processes and microbial degradation in the lake ecosystem, which may blur the source orientation and cause the apportionment overlap (Meyers and Ishiwatari 1993; Lamb et al. 2006; Chen et al. 2019). These deficiencies extremely limited our understanding of the C biogeochemical cycle coupling with the changes of catchment vegetation, soil development, and aquatic productivity in the karst area. Thus, it is essential to know the origin, transport, and burial of organic C in the karst ecosystems along with changes over time as well as their response to climate change or other environmental perturbations, including land degradation (Sironić et al. 2017; Lu et al. 2018).

With the rapid development of advanced analytical techniques, such as fluorescence excitation-emission matrix (EEM), high-performance size exclusion chromatography (HPSEC), nuclear magnetic resonance (NMR), etc., they have been successfully employed to explore the chemical and molecular composition of bulk OM from various natural sources (Chin et al. 1994; Coble 1996; Santín et al. 2009; Derrien et al. 2017), thus providing frameworks for the global C cycle (Stedmon and Markager 2005; Lu et al. 2018). As the major OM constituent, humic substances (HS) represent the refractory products derived from the degradation of biomass detritus and are often considered a vital C sink for a longer residence time of several hundred years (Wolfe et al., 2002). Therefore, these fairly recalcitrant copolymers have received increasing attention in view of the terrestrial C sink (Hayes and Clapp 2001; Nguyen and Hur 2011; Derrien et al. 2017). HS are generally fractionated into the hydrophobic and hydrophilic constituents or humic acid (HA), fulvic acid (FA) and humin, etc., according to their polarities or solubility, (Hayes and Clapp 2001; Wang et al. 2009; Derrien et al. 2017). Substantial differences in HS characteristics could exist between those HS subcomponents as well as among different HS origins (Wang et al. 2009; Derrien et al. 2017). For example, soil-derived HS are mostly composed of lignin and condensed aromatic C compared with those from sediment (Hur et al. 2009; Nguyen and Hur 2011; Derrien et al. 2017). Meanwhile, autochthonous HS often contain a higher proportion of H and N in the presence of proteins, lipids, and carbohydrates (Meyers 1994; Trickovic et al. 2007). Hence, the chemical heterogeneity of HS in various environmental compartments from the same basin can help to track the origin and fate of OM, even terrestrial C dynamics at a large scale (Artinger et al. 2000; Hayes and Clapp 2001; Santín et al. 2009; Derrien et al. 2017).

Based on the above considerations, a small catchment—The Lake Hongfeng catchment was selected as a case study in Southwestern China. This catchment characterized by a typical karst topography is an area of concern due to its high rates of soil erosion, annually 46.6 t ha^{-1} a^{-1}, and has been intensively studied by the scientific community in recent decades (Wang et al. 2008; Jiang and Ji 2013; Luo et al. 2019). Sporadic researches on the bulk OM compositions and their transportation across the water, suspended particles, and surface sediment have been investigated early (Wang et al. 2009; Wang et al. 2012; Jiang and Ji 2013). Yet, questions remain about the roles of soil types and erosion intensity on the composition, source, and fate of terrestrial C eroded from terrestrial to aquatic systems. In the present work, we compared the spectroscopic properties and molecular compositions of different OM components in this studied area, especially HS extracted from surrounding topsoil and sediments. ^{13}C isotopic signatures along with elemental ratios were also employed to explore the source of bulk OM in sediments. The goals of this study were (1) to analyze similarities and differences in the structural and chemical characteristics of OM subcomponents or HS fractions in various environmental media; (2) to identify the primary OM sources in sediment cores; (3) to explore the coupling relationship between the transfer, burial

processes of organic C and past regional eco-environmental changes, particularly soil erosion in this catchment.

Materials and methods

Site description

The Lake Hongfeng catchment is located at the center of the Guizhou Karst Plateau with a drainage area of 1596 km^2 (Fig. 1). Permian and Triassic limestone, dolomite, sandstone, and sandy shale are extensively occurs in this catchment (Wan 1999). Three primary soil types underlie here, i.e., yellow soil, paddy soil, and calcareous soil, which constitute 42.2%, 23.8%, and 22.7% of the total area, respectively. Ground cover has changed significantly since the construction of the lake, and the original subtropical evergreen and deciduous broadleaved forest have been largely replaced by secondary and plantation forests (Luo et al. 2019). Present land uses mainly consist of farmland, forestland, paddy field, shrubland, and grassland. In particular, farmers have cultivated farmlands on slopes to meet population demand, with a land reclamation rate of up to 40% (Zhang et al. 2014a). This studied area is characterized by the subtropical monsoon climate with a mean annual temperature of 14 °C and 1200 mm of precipitation. More than 80% of rainfall occurs from April to October. Consequently, thin soil patches on the sparsely vegetated and rugged slopes are easily washed away by heavy seasonal rainfall (Wang et al. 2012). This catchment is very vulnerable to soil erosion due to its fragility.

Lake Hongfeng (N 26° 26–36′, E 106° 19–28′) situates in the upper drainage basin of River Maotiao, which is an important branch of Yangtze River (Fig. 1). As the largest artificial freshwater lake in Guizhou Karst Plateau, it was built in 1960 and supplied 4 × 10^5 m^3 of daily drinking water for Guiyang City, the capital of Guizhou Province. It has a surface area of 57.2 km^2, average depth of 9.3 m (max. 45 m), and capacity of 6 × 10^8 m^3 (Wang et al. 2012). It is monomictic, and seasonic anoxic in the hypolimnion from late spring to early autumn each year. It suffered from eutrophication and cyanobacterial blooms from 1994 to 2007 because of the high nutrients input, as a result of rapid urbanization and industrialization development in this catchment (Long et al. 2018). After the external nutrient loading has been steadily controlled, alga blooms declined. Till now, it is a mesotrophic water body with average concentrations of total nitrogen (N) and phosphorus (P), and chlorophyll *a* (Chl-*a*) around 1.55 mg L^{-1}, 0.03 mg L^{-1}, and 20 μg L^{-1}, respectively (Qianqiu 2019).

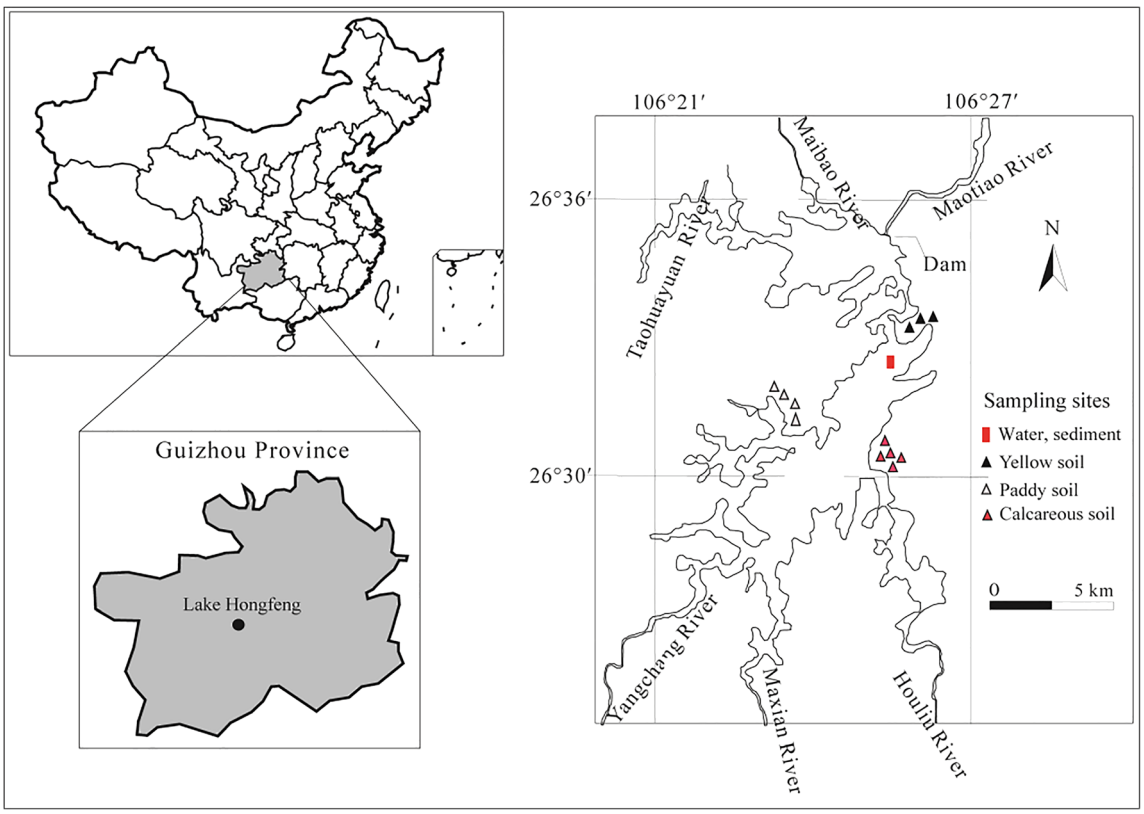

Fig. 1 Location of Lake Hongfeng Catchment and the sampling sites

Sample collection

Three typical soils, namely yellow soil, calcareous soil, and paddy soil, were sampled at the upper 15 cm from the adjacent area, after removing the litter covering on the soil surface in July 2014. Specifically, yellow soil samples were collected from the coniferous forest with shrub. Calcareous soils were sampled in a block of fallow land with sparse meadow nearby the Houliu tributary. Paddy soils were collected during the tillering stage in the rice field from a local farm. For each sampling site, 3–5 different soil subsamples were collected at random within a 10-m^2 plot and then combined in the field to form a representative composite sample. Prior to the lab analysis, visible root residues and stones were removed from each sample manually. All soil samples were gently crushed to pass 2-mm mesh sieves in the laboratory.

A large volume of lake water (approximately 1000 L) was collected under the water surface 1 m at the lake center (N 26° 32′ 45.9″ E, 106° 25′ 45.5″), adjacent to the intake of the Guiyang Xijiao Waterwork. Physio-chemical parameters, including water temperature (T), dissolved oxygen (DO), and Chl-*a*, were measured in situ by a multi-sensor sonde (YSI 6600, Yellow Springs Inc, USA). Water sample was immediately filtered through a 0.45-μm membrane for the next analysis.

Two sediment cores were retrieved synchronously at the same sampling site using a gravitational sampler. Both cores were 48 cm thick and then sliced into 4 sections of 0–10 cm, 10–20 cm, 20–30 cm, and 30–48 cm by depth in the field. Samples were taken back to the laboratory quickly, together with the above-filtrated waters. Sediments were further lyophilized, homogenized, and powdered to 0.15 mm.

Fractionation of OM in different environmental samples

Soil OM was extracted followed a modified International Humic Substances Society (IHSS) standard procedure detailed elsewhere (Swift 1996; Derrien et al. 2017). Briefly, soil sample was pretreated by 0.1 mol L^{-1} HCl solution to remove carbonates. The supernatant then flowed through the XAD-8 resin column and flushed to collect FA. The effluent was acidified again, added 0.3 mol L^{-1} HF, and then passed a H^+ saturated exchange resin column (Bio-Rad AG-MP-50). The solid residues were neutralized and agitated in 0.1 mol L^{-1} NaOH solution under a N_2 atmosphere protection. The supernatant was separated by centrifugation, acidified to pH = 1, and stood overnight to precipitate as raw HA. After dissolving it in a mixed solution of KOH and KCl, it was centrifuged again to remove residual clay minerals. The supernatant was conducted repeatedly following the above steps, then were treated by a mixture of 0.1 mol L^{-1} HCl and 0.3 mol L^{-1} HF to eliminate the impurities, and dialyzed against distilled water. The purified HA and FA were freeze-dried, ground, and stored in a desiccator.

Dissolved OM in the overlying water of Lake Hongfeng were fractionated into six fractions according to the protocol of Wang et al. (2009), i.e., HA, FA, hydrophobic neutrals (HON), hydrophilic acids (HIA), hydrophilic bases (HIB), and hydrophilic neutrals (HIN) based on their polarities. These OM subcomponents were further concentrated by rotary evaporation at 40 °C then dialyzed and freeze-dried like the purification of soil HA and FA.

Prior to extracting sedimentary OM, samples were also pretreated with 0.1 mol L^{-1} HCl solution and then extracted with 0.1 mol L^{-1} NaOH solution for 24 h at room temperature (Fuse et al. 2016; Derrien et al. 2017). The extracted solution was acidified to below pH 2.0 to precipitate HA, while the supernatant was centrifuged to collect FA. The solid residue was regarded as humin. The as-obtained HA and FA were continuously purified in the same manner as soil HS. These HS subcomponents were then lyophilized for further analysis.

Analysis and characterization

Basic physicochemical properties of water, soil, and sediment samples in the Lake Hongfeng Catchment

For the determination of soil moisture content, about 20 g of fresh crushed soil was tightly packed into an aluminum box. The weight loss was calculated when dried at 105 °C to a constant weight (Zhang et al. 2014a). Soil pH in the aqueous solution was measured using the acidity meter (pH 3C, Shanghai, China) after agitation for 30 min. Dissolved organic carbon (DOC) concentrations of six fractions were determined by high-temperature catalytic oxidation at 680 °C using an analyzer (Elementar High TOC II, Germany) with a detection limit of 0.2 mg L^{-1}. The potassium hydrogen phthalate dissolved in ultra-pure water (18.2 Ω) was used as the standard to analyze DOC. The water content of sediment was evaluated by mass loss during freeze-drying.

Elemental composition, spectrometric, and molecular analyses of various OM fractions

Elemental compositions (C, H, N, and S) were measured for six dissolved OM fractions, bulk soil, sediment samples, and HS subcomponents by a CHNS Vario elemental analyzer. The relative content of oxygen (O) for those samples was calculated by subtracting the percentages of C, H, N, and S. The reproducibility was in the range 0.1–0.2 wt. % for C and better than 0.03 wt. % for N. Total C yields in samples were calculated by the C contents sum of individual OM components. Furthermore, the atomic ratios of C/H, O/C, and C/N were estimated on the basis of their relative contents. Generally, C/H often reflects the unsaturation degree of hydrocarbons

(Wang et al. 2009). The higher O/C ratio implies the greater content of O-containing functional groups. The ratio of C/N is usually regarded as an indicator of OM sources in a lake (Lamb et al. 2006).

UV-Vis absorbance is widely applied to investigate OM optical properties in natural water and soil (Chin et al. 1994; Hur et al. 2009). The UV absorption at 254 nm ($SUVA_{254}$) was often deployed to deduce the relative proportion of aromatic structures in samples (Peuravuori and Pihlaja 1997). Likewise, the UV absorptions at 280 nm ($SUVA_{280}$) can provide valuable information for the aromaticity degree, humification extent, and the molecular weight (Chin et al. 1994). The above six kinds of dissolved OM fractions, soil, and sedimentary HS solutions were placed in a 1 quartz cell, and scanned in the range of 200–700 nm with a UV-VIS spectrophotometer (T6 model, New Century Co., Beijing). $SUVA_{254}$ and $SUVA_{280}$ were determined and normalized by DOC concentration. Moreover, the E_4/E_6 ratio was calculated as the absorption strength at 465 to 665 nm. This value can be used as an index for the degree of humification and aromatic condensation (Stevenson 1994; Senesi et al. 2007).

Fluorescence spectra were recorded with a fluorescence spectrometer (Hitachi, Model F-4500, Japan). The excitation (*Ex*) wave lengths fitted from 220 to 400 nm at a 2-nm interval, and the emission (*Em*) wavelengths from 250 to 550 nm at a 5-nm increment. Slits and scan speed setting referred to the procedure of Wang et al. (2009). Ultra-pure water was measured as a blank and subtracted from sample signals. EEM spectra were processed using the software Sigma Plot 2000 (SPSS) and the fluorescence intensity was expressed in arbitrary unit (a.u.). Fluorescent constituents in samples were identified on the basis of published data (Coble, 1996; Yamashita and Jaffé 2008; Huguet et al. 2009). For EEM spectra of natural OM, two fulvic-like fluorescence were generally categorized as the terrestrial origin (Coble 1996; Yamashita and Jaffé 2008), while two protein-like fluorescence were congruent with tyrosine-like and tryptophan-like fluorophores that were mostly produced by autogenous microbe and phytoplankton (Zhou et al. 2015; Lü et al. 2019). Additionally, the fluorescence index (FI) and the freshness index (BIX) were determined as the source and compositional index of dissolved OM (Huguet et al. 2009; Wang et al. 2009). Higher FI (ca. 1.8) usually refers to autochthonous OM, whereas lower FI (ca.1.4) represents the terrestrial source (Fellman et al. 2010). BIX is used to characterize the relative contribution of autochthonous OM to the water body. This index ranged from 0.6 to 0.8, indicating the prevailing terrestrial source. If it exceeded 1.0, this reflected the autochthonous OM source (Huguet et al. 2009).

Molecular weight distribution was measured by HPSEC with a UV detector at 254 nm in the same manner described previously (Wang et al. 2009). OM subcomponents were dissolved in a phosphate buffer solution (pH = 6.8) as the mobile phase with a final C concentration of 10 mg L^{-1}. The weight averaged molecular weight (*M*w), number-averaged molecular weight (*M*n), and polydispersity (ρ) were also determined (Wang et al. 2009).

Stable isotopic analysis

Carbon isotopic measurements were carried out on all homogenized samples after the removal of inorganic C. Approximately, a 3-mg sample was sealed into a tin capsule and combusted in excess oxygen at 1050 °C using an elemental analyzer (Thermo Quest). Residual oxygen was eliminated through reaction with reduced Cu at 600 °C followed by a H_2O trap, and then the resulting CO_2 was analyzed by a micromass isotope ratio mass spectrometer (Isoprime, GV Instruments, UK) on line. The ^{13}C isotope ratio was calibrated with the Pee Dee Belemnite standard. The reproducibility of $\delta^{13}C$ analysis was 0.3‰ for the entire process.

The contributions of different OM sources

Based on the above C/N and δ^{13} signatures of different OM end-members, the feasible contributions of several potential sources to sedimentary OM were quantified roughly using the linear mixing models (Phillips 2001), as follows the equations:

$$\left(\frac{C}{N}\right)_{sample} = \sum_{i=1}^{n}\left(\frac{C}{N}\right) i \times f_i$$

$$\delta^{13}C_{sample} = \sum_{i=1}^{n} \delta 13Ci \times f_i$$

$$\sum_{i=1}^{n} fi = 1$$

where C/N is the atomic ratio of carbon to nitrogen in samples and end-members (*i*), $\delta^{13}C$ is their stable carbon isotopes (*i*), and *f* represents the relative contribution of each end-member (*i*).

Results

Water quality characteristics and basal physicochemical properties of the studied samples

The results showed that the yellow soil was slightly acidic, whereas the calcareous soil and paddy soil were nearly neutral in this catchment (Table 1). Their moisture contents were almost equal. The paddy soil was composed of the highest contents of organic C and TN, followed by the calcareous soil and yellow soil. The C/N ratios of three soil types varied from 12.18 to 15.20, and corresponding $\delta^{13}C$ values ranged from − 26.76 to − 20.10‰.

Table 1 The basic physicochemical properties of the studied soils and sediments

Samples		pH	Water content	Elemental composition (wt%)					C/N*	$\delta^{13}C$
			(%)	C	N	H	S	O		(‰)
Soils	Yellow soil	4.86–5.75	23.5	1.50	0.12	1.69	0.77	95.93	15.20	− 20.10
	Calcareous soil	6.89–7.06	22.4	3.75	0.31	1.39	0.62	93.94	14.34	− 26.76
	Paddy soil	6.77–7.18	24.6	4.62	0.44	1.58	0.93	92.44	12.18	− 25.86
Sediments	HF-10		88.5	5.78	0.66	1.59	4.09	87.88	10.22	− 27.87
	HF-20		77.8	4.43	0.40	1.18	2.12	91.87	12.92	− 27.45
	HF-30		68.6	2.73	0.30	0.95	0.69	95.33	10.62	− 26.13
	HF-48		57.0	2.32	0.27	1.36	0.63	95.42	10.02	− 25.93

*The atomic ratio of C to N

In Lake Hongfeng, water quality parameters such as T, DO, and Chl-*a* exhibited distinct stratification at a 12-m depth in summer (Fig. 2). This trend was also expressed visually by the profile change of DOC, and its concentration in the surface layer was three times higher than the bottom water.

The water content of sediment decreased gradually throughout the core profile. Accumulation of organic C was greater in the surface 10-cm sediment than that in those topsoil and dropped dramatically with the sediment depth. The C/N ratios in the sediment core varied in the low range of 10.02 to 12.92 compared with those of soils, while their $\delta^{13}C$ values were somewhat negative.

Elemental composition and spectrometric and molecular weight of six kinds of dissolved OM fractions, soil, and sedimentary HS

Elemental composition, atomic ratios, and $\delta^{13}C$ values of these OM subcomponents were listed in Table 2. The organic C content of soil HA was ranked in the order of yellow soil < paddy soil < calcareous soil, in agreement with the parent soils. The C/H, O/C, and C/N ratios for soil HA fractions varied from 0.79 to 0.99, from 0.75 to 1.07, and from 10.37 to 14.44, respectively. Their corresponding $\delta^{13}C$ values were close to that of dissolved OM fractions. Unfortunately, elemental composition analysis of soil FA and its C recovery estimation cannot be conducted in this study due to the insufficient extraction from bulk soil samples.

For six fractions of dissolved OM, the C proportions of the hydrophobic fractions were significantly higher than those of the hydrophilic fractions. Among them, the N content of FA was detected the lowest, whereas the H proportion of HON was observed highest. The C/H ratios of those dissolved OM constituents varied slightly, from 0.58 to 0.81. The O/C ratios of the hydrophobic components were markedly less than those of the hydrophilic components. The C/N ratios of HA and FA were greater than 14, while those of the other four fractions fluctuated around 10. Their $\delta^{13}C$ ranges slightly differed, from − 26.80 to − 25.64‰.

The proportion of HS in sedimentary OM varied from 23.5 to 45.8%, based on the estimation of their organic C contents. Among them, HA, FA, and Humin constituted 62–87%, 10–

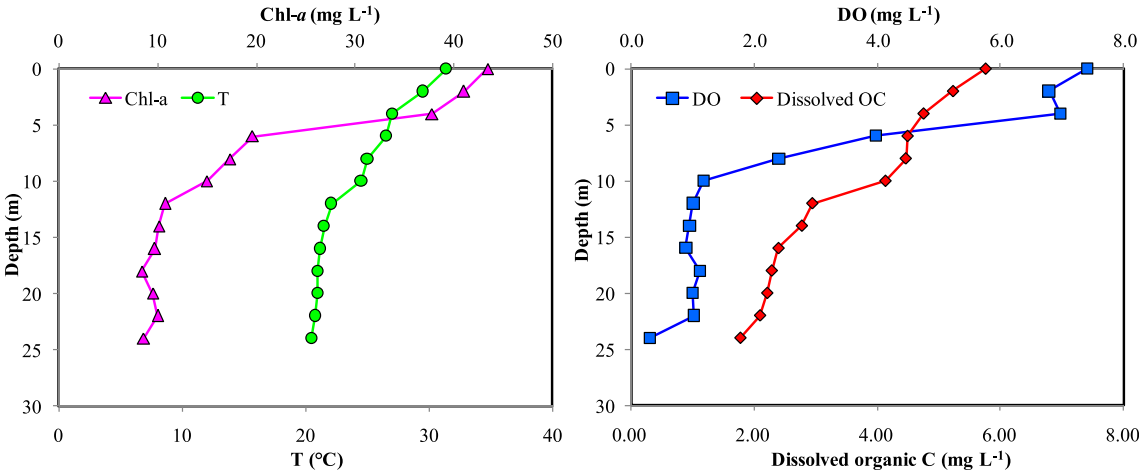

Fig. 2 Vertical distributions of water quality parameters of T, Chl-*a*, DO, and concentrations of dissolved organic C in the water column of Lake Hongfeng

23%, and 3-15%, respectively. For sedimentary HA, the highest C content was found in the surface 10-cm layer and changed marginally below this depth. Nevertheless, the C contents of FA and humin decreased throughout the profile. Their C/N ratio ranges were 8.3–12.2, 11.82–15.03, and 21.00–39.74, and the corresponding $\delta^{13}C$ varied from − 28.25 to − 24.87‰, from − 27.42 to − 24.33‰, and from − 26.24 to − 22.34‰, respectively.

The spectra of all OM subcomponents appeared no characteristic at absorption peaks, and the absorption intensity decreased with the increasing wavelength (Table 3). The $SUVA_{254}$ and $SUVA_{280}$ values of six kinds of dissolved OM constituents ranged from 1.70 to 2.96 L (mg C m)$^{-1}$ and from 1.03 to 2.09 L (mg C m)$^{-1}$, while the E4/E6 ratio varied in the range of 3.20–7.50. These results were markedly lower than those of most soil and sedimentary HS in this catchment.

EEM spectra of those OM subcomponents were presented in Fig. 3. Five distinct fluorophores were discerned, i.e., two fulvic-like fluorescence including UV fulvic-like peak A (*Ex,* 230–260 nm; *Em*, 420–460 nm) and visible fulvic-like peak C (*Ex*, 300–330 nm; *Em*, 420–450 nm), two protein-like fluorescence, peak B (*Ex* 275–290 nm; *Em* 330–360 nm) and peak D (*Ex* 220–250; *Em*, 340–370 nm), and one humic acid-like peak E (*Ex*, 420–440; *Em*, 480–510 nm). Considerable differences of fluorescence spectra between soil HA and FA were observed among the three studied soil types. Specifically, both the yellow soil HA and FA embodied a fulvic-like peak and protein-like peak. In contrast, UV fulvic-like peak A and humic-like peak E appeared in the HA fraction of the paddy soil and calcareous soil, while two typical fulvic-like peaks were present in the corresponding FA fraction (Fig. 3, Table 4). For the dissolved OM constituents, only peak A was found in HA, a protein-like fluorescence in HON, while two kinds of fulvic-like peaks existed in the other four components. Additionally, FI and BIX values of six dissolved OM constituents varied from 1.10 to 1.62 and from 0.62 to 0.85. The fluorescence spectroscopy of sedimentary HA and FA were quite similar to those of the calcareous soil and the paddy soil, and the peak intensity decreased with the sediment depth.

The estimated *M*w, *M*n, and ρ value of those OM subcomponents are summarized in Table 5. Interestingly, the molecular weight of calcareous soil HA and FA were much larger than those of the yellow soil and paddy soil. Six dissolved OM

Table 2 Elemental compositions, atomic ratios, and $\delta^{13}C$ values of six dissolved OM fractions, HS extracted from the studied soils and sediments

Samples		Elemental composition (wt%)					C/H*	O/C*	C/N*	$\delta^{13}C$
		C	N	H	S	O				(‰)
Soil HSs	Yellow soil HA	37.96	4.27	3.2	0.26	54.31	0.99	1.07	10.37	− 25.44
	Calcareous soil HA	43.74	4.04	4.64	0.33	47.25	0.79	0.81	12.63	− 26.22
	Paddy soil HA	45.78	3.7	4.57	0.29	45.66	0.83	0.75	14.44	− 25.63
Dissolved OM fractions	HA	43.40	3.50	4.45	1.01	47.64	0.81	0.82	14.47	− 26.80
	FA	35.36	1.50	3.68	0.66	58.81	0.80	1.25	27.50	− 25.71
	HON	46.20	5.15	7.64	0.85	40.16	0.58	0.65	10.47	− 26.36
	HIA	30.27	3.03	3.24	0.17	63.29	0.78	1.57	11.66	− 26.62
	HIB	31.11	3.50	4.31	0.36	60.72	0.60	1.46	10.36	− 26.54
	HIN	33.90	3.70	3.83	0.05	58.53	0.74	1.29	10.69	− 25.64
Sedimentary HSs	HA-10	48.15	6.77	6.23	0.53	38.32	0.64	0.60	8.30	− 27.42
	HA-20	36.54	4.26	5.00	0.49	53.71	0.61	1.10	10.01	− 25.90
	HA-30	38.36	4.24	4.73	0.43	52.24	0.68	1.02	10.56	− 25.16
	HA-48	36.49	3.49	4.21	0.39	55.42	0.72	1.14	12.20	− 24.33
	FA-10	7.47	0.58	2.08	0.25	89.62	0.30	9.00	15.03	− 27.75
	FA-20	6.25	0.54	0.99	0.07	92.15	0.53	11.06	13.50	− 27.42
	FA-30	6.09	0.59	1.77	0.16	91.39	0.29	11.25	12.04	− 26.16
	FA-48	3.75	0.37	1.32	0.17	94.39	0.24	18.88	11.82	− 24.87
	Humin-10	5.13	0.23	0.47	0.00	94.17	0.91	13.77	26.02	− 26.24
	Humin-20	3.54	0.13	0.66	0.04	95.63	0.45	20.26	31.77	− 25.66
	Humin-30	2.18	0.06	0.65	0.05	97.06	0.28	33.39	39.74	− 25.10
	Humin-48	1.80	0.10	0.69	0.05	97.36	0.22	40.57	21.00	− 22.34

*The atomic ratio of individual element

Table 3 Specific UV absorbance [L (mg C m)$^{-1}$] at 254 nm, 280 nm and the E4/E6 ratios of six dissolved OM fractions, HS extracted from the studied soils and sediments

Samples		$SUVA_{254}$	$SUVA_{280}$	E4/E6
Soil HS	Yellow soil HA	4.57	4.08	4.50
	Calcareous soil HA	6.74	5.00	3.73
	Paddy soil HA	6.53	5.97	4.96
	Yellow soil FA	2.28	1.97	6.65
	Calcareous soil FA	2.40	1.73	4.72
	Paddy soil FA	3.93	1.73	7.43
Dissolved OM fractions	HA	1.88	1.49	3.75
	FA	2.43	1.60	7.50
	HON	1.70	1.03	4.60
	HIA	2.50	1.65	5.25
	HIB	2.96	2.09	4.83
	HIN	1.50	1.06	3.20
Sedimentary HS	HA-10	3.97	3.53	4.38
	HA-20	7.28	6.47	4.02
	HA-30	7.41	6.76	4.01
	HA-48	9.54	8.51	3.00
	FA-10	2.53	1.99	7.60
	FA-20	2.29	1.67	6.67
	FA-30	3.33	2.44	4.83
	FA-48	4.09	2.56	4.50

fractions had a narrow molecular weight range (*M*w, 1765-2674 Da; *M*n, 1429–2049 Da), and the hydrophobic fractions had a larger molecular weight and ρ values than that of the hydrophilic fractions. In addition, the molecular weight distribution of sedimentary HS was similar to that of soil HS, with relatively higher ρ values for the FA fraction.

Estimation of contributions of OM sources in lake sediment

Based on the C/N ratios and $\delta^{13}C$ assigned to different end-members, plots of sedimentary OM are situated far from the signatures of land-derived C4 plants (Fig. 4). Therefore, it was presumed that the contribution of terrestrial C4 plants can be ignored in the OM source apportionment. Accordingly, the distinct features of three environmental end-members were used in the isotopic multivariate mixing model: (1) Earlier investigation of phytoplankton data (C/N 8.0, $\delta^{13}C$ − 30.00‰) from this lake was adopted (Li, 2009). (2) Actual measurement of surrounding soils (C/N 13.90, $\delta^{13}C$ − 24.24‰) was used, as the mean values of three kinds of soil types in this catchment. (3) Terrestrial C3 plants (C/N 20, $\delta^{13}C$ − 27‰) referred to the average of the empiric value (Kendall and Coplen 2001). It was estimated that the contribution of terrestrial soil and C3 plants was 56.3% and 3.7%, respectively, whereas phytoplankton accounted for 40.0% of sedimentary OM.

Discussion

Soil OM and associated HS characteristics

Remarkable differences of organic C content were observed between the calcareous soil and the other two soil types in this catchment (Table 1), which were consistent with previous reports (Zhu et al. 2007; Di et al. 2019). In the context of karst landform, the calcium content of the calcareous soil was approximately one order magnitude higher than that of the yellow soil (Di et al. 2019). Thus, soil OM, particularly HA, can be preserved in the form of Ca^{2+}-OM complexes and/or co-precipitate with hypergene $CaCO_3$, thus hard to biodegrade and lose (Di et al., 2019). However, yellow soil OM is tightly bound to R_2O_3 with more leached calcium, resulting in low organic C content (Zhu et al. 2007). Paddy soil is a kind of cultivated soil developed on natural soils and formed by man-made water tillage and flooding. As a result of long-term maturation hydroponics and fertilization management, organic C content was elevated to a certain extent (Wang et al. 2019).

The results of elemental composition analysis showed the lower C/H ratios for the calcareous soil and the paddy soil HA than the yellow soil HA suggesting that they contained more carbohydrate fractions (Table 2). Similar rules were reported whereas the C/H ratios of the calcareous soil and yellow soil HA varied in the range of 0.64–0.68 and 0.73–0.85 in Southwest China (Ma et al. 2016). The ratio of C/N is usually

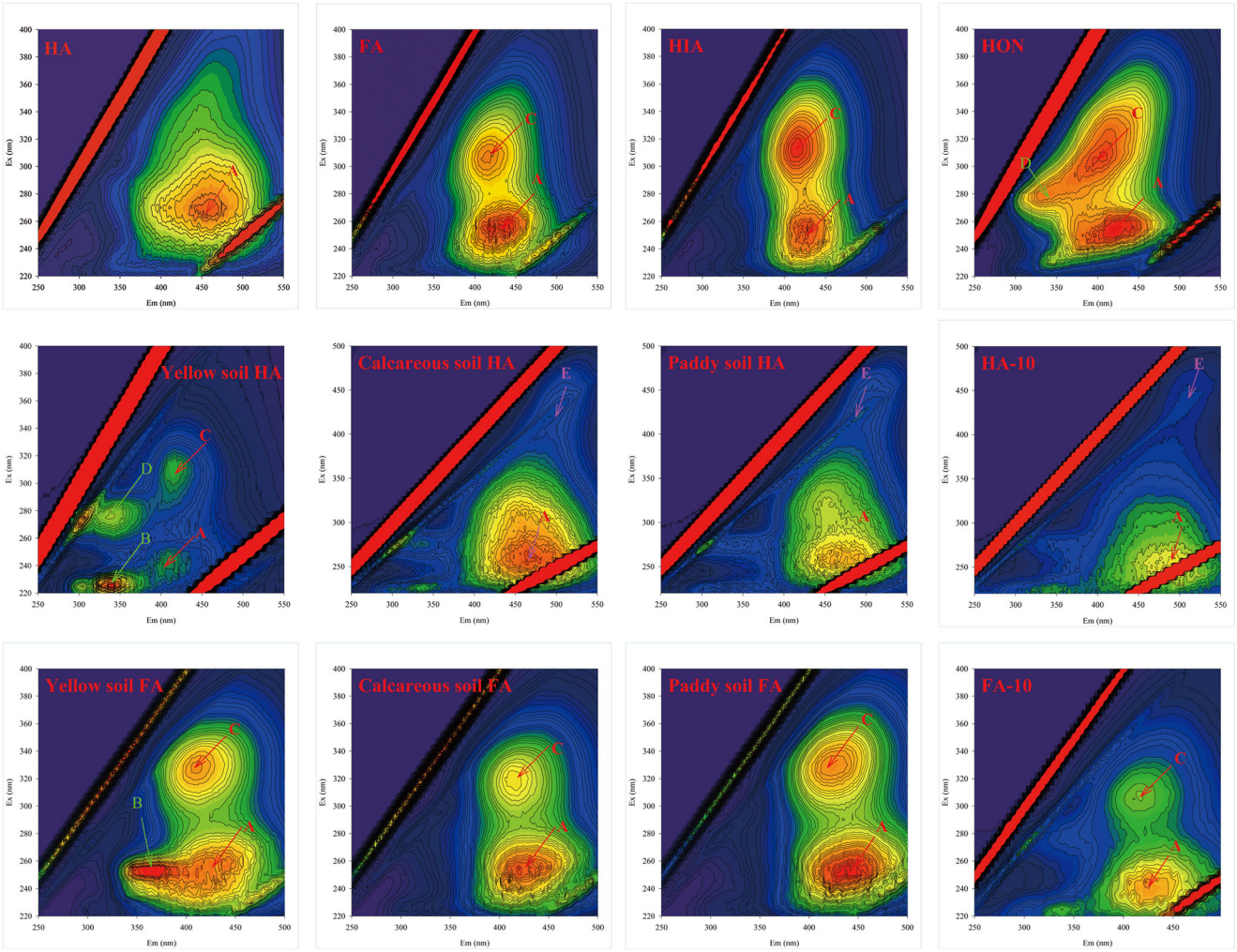

Fig. 3 Typical fluorescence spectra of selected dissolved OM fractions, HS extracted from the studied soils and sediments

analyzed alongside $\delta^{13}C$ to determine the relative contributions of various OM sources in a lake (Lamb et al. 2006). Bacteria, algae, and soil OM generally have low C/N ratio of < 5, 5–10, and 10–15, respectively, which are distinct from those of terrestrial vegetation, such as C3 and C4 plants above 20 (Meyers 1994; Lamb et al. 2006). The $\delta^{13}C$ of some phytoplankton varied from − 12 to − 24‰. If it uses atmospheric CO_2 as the photosynthetic C source, then $\delta^{13}C$ will be depleted and biased to − 35.5‰ (Jiang and Ji 2013; Lu et al. 2018). In contrast, if it utilizes HCO_3^-, $\delta^{13}C$ will be more positive (Wang et al. 2012). The $\delta^{13}C$ of soil OM largely depended on their origin, whether from a C3-dominated environment (light $\delta^{13}C$ value, from − 21 to − 33‰), or froma C4-dominated environment (heavier $\delta^{13}C$, from − 10‰ to − 21‰) (Kendall and Coplen 2001; Goni et al. 2003). In this study, the C/N ratios and $\delta^{13}C$ results indicating soil OM came mainly from the C3 plant source. Pedogenesis was remarkably slow on these parent materials in karst landscape. Soils are usually thinner than 50 cm in Southwest China, only one third to half as thick as those developed on noncarbonate bedrock under similar climate regimes (Jiang et al. 2014; Luo et al. 2016). Hence, a substantial terrigenous organic matter easily entered into this lake during the wet season (Long et al. 2018; Luo et al. 2019).

A notable higher $SUVA_{254}$ and $SUVA_{280}$ values for soil HA were observed than the FA fraction in this catchment (Table 3). Similar results were reported elsewhere (Hur et al. 2009; Derrien et al. 2017). This probably related to the abundance of condensed aromatic structures in the former, which is supported by their C/H ratios mentioned before (Table 2). Usually, lower E4/E6 values (about 3–5) were assigned as high-molecular HA with developed aromatic carbon network and higher (6–10) for low-molecular, young, and more aliphatic FA (Stevenson1994). The E4/E6 ratios of soil HS basically fell in this range in the present study.

As seen in Fig. 3, EEM spectra of the calcareous soil and the paddy soil agreed with previous findings (Santín et al. 2009). However, protein-like peaks were found in the spectra

Table 4 Maximum fluorescence peaks and intensities (I) of six dissolved OM fractions, HS extracted from the studied soils and sediments, and the FI, BIX indexes of dissolved OM fractions

Samples		Peak A	I	Peak C	I	Peak B	I	Peak D	I	Peak E	I	FIa	BIXb
Soil HSs	Yellow soil HA	245/402	145.7	310/413	155.2	225/342	307.7	275/336	188.5				
	Calcareous soil HA	260/468	188.2							425/498	84.34		
	Paddy soil HA	262/472	160.3							420/492	86.63		
	Yellow soil FA	255/444	708.4	330/412	675.2	250/368	843.8						
	Calcareous soil FA	253/420	1039	320/414	798.1								
	Paddy soil FA	255/440	1208	330/426	1010								
Dissolved OM fractions	HA	265/456	570.7									1.15	0.62
	FA	255/434	799.0	305/418	689.4							1.22	0.65
	HON	250/422	1636	305/410	1531			280/346	1413			1.62	0.85
	HIA	255/428	794.1	310/414	799.3							1.10	0.63
	HIB	240/414	1406	315/428	996							1.40	0.72
	HIN	240/418	576.8	310/412	723.5							1.42	0.66
Sedimentary HSs	HA-10	265/494	115.3							430/500	77.97		
	HA-20	260/498	109.4							435/508	70.49		
	HA-30	260/498	93.10							435/510	49.09		
	HA-48	260/494	75.27							435/508	31.96		
	FA-10	240/420	275.8	310/416	203.3								
	FA-20	240/424	188.4	310/420	123.8								
	FA-30	245/422	142.6	310/420	92.4								
	FA-48	245/430	128.7	310/424	90.5								

[a] FI means the ratio of fluorescence intensity at *Em* wavelength 450 nm to that of at 500 nm at a fixed *Ex* wavelength of 370 nm

[b] BIX is estimated as the ratio of the emission intensity at 380 nm divided by the maximum emission intensity between 420 and 435 nm, at an *Ex* 310 nm

of the yellow soil associated HA and FA, owing to the abundance of N-containing constituents. Its low pH value can promote acidic hydrolysis of soil OM to some N-containing constituents, such as proteins, nucleic acids, and polysaccharides (Di et al. 2019). Additionally, humic-like peak E is presented in the paddy soil and the calcareous soil HA (Fig. 3; Table 4). This fluorophore was designated as the terrestrial OM, which has been detected in IHS HS and the HA fraction extracted from estuarine soils of the Iberian Peninsula (Yamashita and Jaffé 2008; Santín et al. 2009).

Because of the formation of Ca^{2+}-OM complexes or co-precipitate with hypergene $CaCO_3$ in calcareous soil, the *M*w, *M*n of both HA and FA fractions were notably larger than that of the yellow soil and the paddy soil (Table 5). This indicated that the chemical composition of soil OM is closely related to the lithology. Ma et al. (2016) pointed out that general molecular weight distributions of HA of the calcareous soil and yellow soil in Southwestern China were similar by ultrafiltration; however, the size distributions in those two HA remain notably different. Furthermore, the large molecular fractions (> 50 kD) occupied about 70 wt% and 91 wt% of those two soil HA, respectively.

Concentrations of DOC and characteristics of six fractions of dissolved OM

The average DOC concentration at the lake center was 3.48 ± 1.33 mg L^{-1} (Fig. 2), which was slightly higher than previous results (Wang et al. 2009; Wang et al. 2012). But it was far less than the median value of 5.71 mg L^{-1} documented from global lakes (Sobek et al. 2007) and the mean value of Yun-Gui Plateau lakes (7.0 mg L^{-1}), Southwest China (Song et al. 2018). In karst surface water, DOC mainly originated from phytoplankton via photosynthetic uptake of carbonate weathering inorganic C (Jiang and Ji 2013; Lu et al. 2018). Prior results show that the export load ratio of inorganic and organic C is up to 21 in this studied area, indicating that over 95% of terrestrial C export existed in the form of HCO_3^- in Lake Hongfeng (Wang et al. 2012). Relevant investigation found that HS amounted to 64% of dissolved OM in this lake, and FA contributed to 51% (Wang et al. 2009). The presence of a high percentage of hydrophobic fractions could be closely related to plenty allochthonous OM input, due to the severe soil erosion and strong runoff in this catchment. It was reported that the soil loss area is up to 311.5 km^2, accounting for 20.2% of the drainage area (Jiang and Ji 2013).

Table 5 Molecular weight distribution ranges and ρ values of six dissolved OM fractions, HS extracted from the studied soils and sediments

Samples		*Mw* (Da)	*Mn* (Da)	ρ
Soil HSs	Yellow soil HA	5445.94	4870.25	1.12
	Calcareous soil HA	6249.32	5144.04	1.21
	Paddy soil HA	5412.84	4921.68	1.10
	Yellow soil FA	2200.33	1792.61	1.22
	Calcareous soil FA	2954.39	2242.26	1.32
	Paddy soil FA	2732.71	2104.11	1.29
Dissolved OM fractions	HA	2674	2049	1.31
	FA	2232	1546	1.44
	HON	2199	1652	1.33
	HIA	1852	1461	1.27
	HIB	1871	1603	1.17
	HIN	1765	1429	1.24
Sedimentary HS	HA-10	6049.04	5833.17	1.04
	HA-20	5828.11	5538.54	1.05
	HA-30	5857.70	5485.39	1.07
	HA-48	5670.93	5398.90	1.05
	FA-10	2475.16	1728.37	1.43
	FA-20	2311.30	1613.98	1.43
	FA-30	2318.39	1534.09	1.51
	FA-48	2305.93	1629.58	1.42

Mw, the weight-averaged molecular weight; *Mn*, the number-averaged molecular weight; ρ, refers to the polydispersity

According to the larger C/H ratios of FA and HA (Table 2), the unsaturation degree was somewhat higher than that of other components. Thus, the hydrophilic components and FA contained more such functional groups compared with HA and HON. The C/N ratios and $\delta^{13}C$ results of dissolved OM fractions in Lake Hongfeng reflected a blend of allochthonous and autochthonous sources. Among them, HA and FA were mainly from terrestrial C3 plant debris, whereas other OM constituents were in situ produced by photosynthetic phytoplankton. Freshwater algae often have lower C/N ratios due to higher protein contents, meanwhile terrestrial high plants have higher C/N ratios because of containing cellulose, lignin, and tannins (Meyers 1994).

The $SUVA_{254}$ and $SUVA_{280}$ values of HON and HIN were markedly lower than those of other components (Table 3), indicating a lower aromatic structure and humification degree and the small molecular weight range for these neutral fractions (Wang et al. 2009). Generally, OM derived from aquatic algae and bacteria had a lower SUVA value than those from terrestrial sources (Wang et al. 2009; Traversa et al. 2014). This finding supported that these dissolved OM constituents were formed by in situ from algal biomass and microbiological activity in Lake Hongfeng.

EEM spectra indicated that most dissolved OM constituents originated from terrestrial sources in this catchment (Fig. 3), which were consistent with the above elemental composition results shown. On the contrary, Lü et al. (2019) found that protein-like components were dominant in a eutrophic lake throughout the entire year. Additionally, the FI values of five dissolved OM fractions varied in the range of 1.10–1.42,

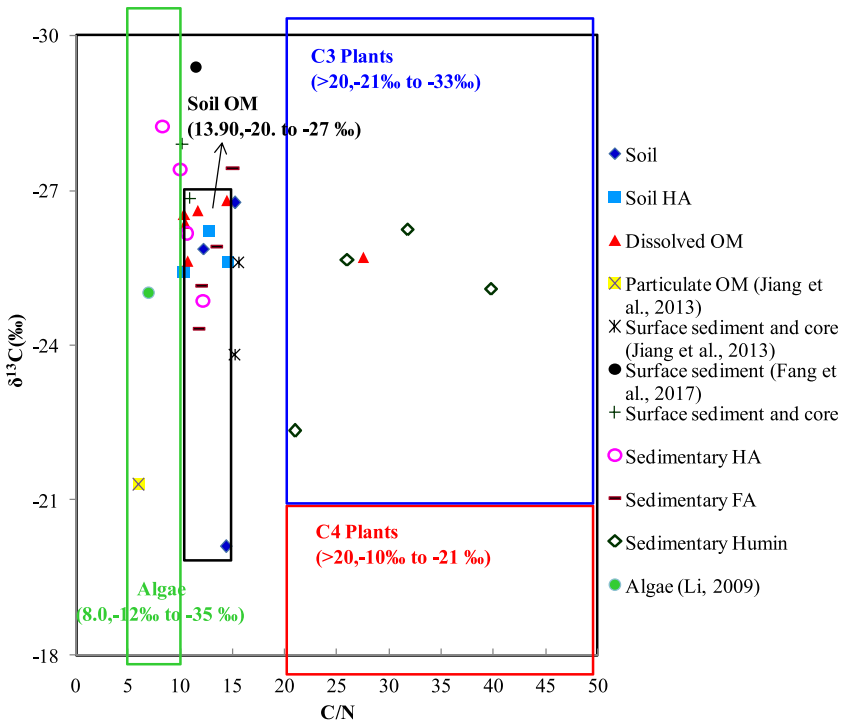

Fig. 4 $\delta^{13}C$ values plotted against atomic C/N ratios of dissolved OM fractions, HS isolated from the studied soils and sediments, and the different end-members including particulate OM, algae, sediment, soil OM, and C3 and C4 plants in the Lake Hongfeng Catchment compiled from previous studies (Zhu et al., 2007; Li, 2009; Jiang and Ji, 2013; Fang et al., 2017)

except HON (Table 4), which also implied the dominance of terrestrial OM input. BIX results also coincided with the above argument.

Six kinds of dissolved OM fractions had small molecular weight distributions (< 3000 Da), similar to previous investigations (Wang et al. 2009). These results could be partially explained by strong UV photo-degradation in Southwest China (Wang et al. 2009; Zhou et al. 2015). Another possibility was that the extracellular products of alga detritus caused the increase of smaller organic molecules in the euphotic layer (Trickovic et al. 2007; Lü et al. 2019).

Sedimentary OM and related HS characteristics

Total organic C content in lake sediment depends on the input quantity and conservation capacity of the deposition environment. Benthic activity is usually active in surface sediments, resulting in greater organic C and water content than that in the bottom layer (Table 1). As seen in Table 2, the C/H ratio of sedimentary HA were close to those from Lake Biwa (0.68-0.81), and lower than those of typical freshwater system (0.72–1.09), while the O/C ratios were slightly higher than that of Lake Biwa (0.61–0.89) and most water bodies in China (0.47-0.58) (Zhang et al. 2010; Fuse et al. 2016). It can be deduced that the sedimentary OM in Lake Hongfeng were highly aromatic with more oxygen atom in the sketch structure compared with those of the above freshwater bodies.

During OM settlement and preservation, early diagenesis can lead to the loss of ^{13}C depletion in sediment than the terrestrial source and the decrease of $\delta^{13}C$ toward the deeper layer. It has also been proved that N was usually mineralized preferentially over C in this process, thus resulting in the dramatic change of the C/N ratio in the profile (Meyers and Ishiwatari 1993; Perdue and Koprivnjak, 2007; Chen et al. 2019). However, neither the $\delta^{13}C$ values nor the C/N ratios exhibited the aforementioned trend in this study (Table 2). The same variation tendency was also observed in nearby Reservoir Wujiangdu and Reservoir Puding in the same watershed (Yang 2017). On the whole, the modest increasing down-core trends of $\delta^{13}C$ for sedimentary HS in Lake Hongfeng probably ascribed to the weak early diagenesis and microbial decomposition. It can be further inferred from the C/N ratios that the HA fraction in the surface sediments was primarily attributed to autochthonous OM in past decades (Table 2), while that of the deeper layer originated from the allochthonous OM. Nevertheless, the C/N ratio and $\delta^{13}C$ values of sedimentary FA indicated the predominant contribution of terrestrial OM. Humin results reflected a major C3 plants contribution. Moreover, comparing the whole sediments rather than the isolated HS depleted in $\delta^{13}C$ (Table 1, Table 2) indicated that the HS embodied a more terrigenous nature than their non-humic part (Tremblay and Gagne 2009; Zhang et al. 2014b).

The UV absorption values of sedimentary HA and FA increased with the sediment depth, implying an enhanced humification degree (Table 3). This conclusion was further supported by the opposite profile change of the E4/E6 results (Senesi et al. 2007).

Most interestingly, a great similarity of fluorescence spectra was found between sedimentary HA, FA fractions, and those from the overlying water, nearby calcareous soil and paddy soil (Fig. 3, Table 4). A similar trend was reported in Hur et al. (2014), in which terrestrial humic-like and fulvic-like fluorescence were predominantly present in sediment and soil HA, or aquatic dissolved OM. This agreement may be caused by the more sensitive nature of HS in responding to regional land-cover change in the karst watershed. The molecular weight distribution of sedimentary HA was also comparable with that of soil HA (Table 5). These probably implied that lake sediments can well record the information of soil erosion and runoff input in the karst catchment (Luo et al. 2019). The molecular weight of sedimentary FA was equivalent to that of Lake Martignano, Italy (500–3000 Da) (Calace et al. 2000), and dissolved FA fraction in Lake Hongfeng, and slightly lower than those of three soil types, owing to the insignificant microbial decomposition in the deposition process (Long et al. 2018). The ρ value of sediment HA was close to 1, indicative of a homogeneous, monodispersed system, whereas that of FA about 1.5 reflected a polydispersed system.

Possible mechanisms of the OM cycle involved in the karst catchment

In the Lake Hongfeng Catchment, the contribution of the allochthonous source including soil and C3 plants accounted for 60% of the total OM pool via end-member mixing analysis. However, the estimation may deviate from the actual situation because the values for other end-members from anthropogenic sources, such as industrial wastewater and domestic sewage, were scanty in this study (Kendall and Coplen 2001; Lamb et al. 2006). Furthermore, a meta-analysis of OM features available in the literature across various compartments in this catchment is exhibited in Fig. 4. Except for particulate OM, most data clearly show that the allochthonous source played an important role in the provenance and delivery of OM. The C/N ratios in surface sediments were intermediate between two contrasting autochthonous and allochthonous OM end-members, while terrestrial sources may be the major contributor to that in deeper sediments. This conclusion was in good agreement with preceding studies (Jiang and Ji 2013; Luo et al. 2019).

In fact, most freshwater lakes in subtropical climates are significantly affected by terrestrial inputs, and allochthonous OM often dominated the C balance (Jiang and Ji 2013). First, changes in land-use patterns have to be considered one of the most significant human activities affecting lake organic C

(Anderson et al., 2013). As a predominant component with the moderate reactivity, HA correlated with the stability of soil aggregates as compared with FA and humin, and thus considered a reliable proxy for the soil OM quality (Traversa et al. 2014). Di et al. (2019) found that the calcareous soil had higher contents of total organic C and HA, especially the proportions of encapsulated and interacted HA fractions than those of yellow soil in Southwestern China, which indicated that it could be more vulnerable to rocky desertification once the vegetation cover was destroyed. The cultivation also reduced soil organic C storage in the calcareous soil, subsequently increased the export flux of organic C (Zhang et al. 2014a; Li et al. 2016). This mechanism had been proved by the rice field investigation on a small Dachong area in this studied catchment (Wang et al. 2019). Another possible reason was the mesotrophication state of this lake maintained since 2010 along with relatively low DOC content (Long et al. 2018). Wang et al. (2012) concluded that a short water residence time of approximately 120 d and a large recharge coefficient of 27.9 (the ratio of drainage area to lake water area) were unfavorable to the metabolism of organic C in this lake.

It is evidenced that the stratigraphic variations in organic C content and C/N ratio in the sediment cores can be used to deduce the OM source and past environmental change over time in the catchment (Sobek et al. 2009; Luo et al. 2019). The linear sedimentation rate has been estimated to be 9.3 ± 0.7 mm a^{-1} in Lake Hongfeng by ^{210}Pb and ^{137}Cs dating (Wan 1999). Accordingly, the deposition ages of each sediment layer corresponded to approximately four episodes of 2014–2003, 2003–1992, 1992–1981, and 1981–1960. In the earliest period before 1992, both organic C content and the C/N ratio are rather low below the 20-cm sediment depth (Table 1), suggesting a small amount of terrestrial OM input. This corroborated the relatively low soil erosion rate from 26.8 to 38.5 t ha^{-1} a^{-1} before 1990 (Zhang et al. 2014a; Luo et al. 2019). At that time, this lake was oligotrophic with very low primary productivity. Period 2 represents from 1992 to 2003; organic C and C/N ratios elevated in the segment of 10–20-cm sediment, indicating more terrestrial-derived OM contribution. During this period, many natural forest lands have been turned into dry arable upland and paddy fields. This further intensified soil erosion and C transfer to this lake. The average annual soil loss reached to 57.7 t ha^{-1} a^{-1} in this episode (Luo et al. 2019). Actually, terrestrial characteristics may be evidently archived in the sedimentary HS, as discussed in the earlier section. Meanwhile, massive nutrient loading raised the eutrophic level and eventually led to high organic C sedimentation rates. Sudden deterioration events of water quality, e.g., alga bloom and dead fish in this lake have been reported frequently since 1994 (Long et al. 2018). Period 3 correspond the latest decade, a small steady increase in organic C and decrease of C/N ratio suggested a significant reduction of terrestrial OM flux, along with the water quality improvement after 2007 (Lu et al. 2018).

It has been estimated that the average organic C accumulation rate in sediment from Lake Hongfeng was approximately 29.37 g m^{-2} a^{-1} (Wang et al. 2012), which was distinctly higher than the average value (8 g m^{-2} a^{-1}) of lakes across China (Wang et al. 2018). This distinction implied greater C sequestration in the karst catchment. Coincidently, organic C accumulation rate during the post-1950 in Lake Fuxian, the deepest oligotrophic lake in Southwestern China, was about 6.9 times that for the period of 1910–1950 subject to land-use change, correspondingly 1.06 g m^{-2} a^{-1} in 1910 and 21.74 g m^{-2} a^{-1} in 2017. Land-cover change has significantly increased the allochthonous C export flux, thus amplifying the OC burial in European and American lakes (Anderson et al. 2014). For example, the C burial rate in freshwater lakes of Iowa, USA, even can fetch up to 200 g m^{-2} a^{-1} following agricultural development (Heathcote and Downing 2012). Therefore, the conversion of forested land to agriculture also definitely accelerated soil erosion in this studied catchment, leading to increased production of organic matter and the enrichment of substantial nutrients (Long et al. 2018; Luo et al. 2019). This was supported by the inherent link between sediment HS characteristics to that of adjacent soil. The findings confirmed that OC burial in lacustrine sediments is characterized by comparatively rapid accumulation, particularly in the karst watershed, and a high preservation factor than that in the oceans (Einsele et al. 2001; Cole et al. 2007).

Conclusions

The Lake Hongfeng Catchment was chosen as a case study to unravel the distribution, migration, and transformation of OM in the karst landform, by using spectrometric and chemical analysis. Results have shown that organic C contents of three major soil types and the extracted HA fraction ranked in the order of the paddy soil > the calcareous soil > the yellow soil. The C/N ratios as well as $\delta^{13}C$ values of the bulk OM characteristics and associated HS fractions reflected the overwhelming contribution of the allochthonous source to the autochthonous source, in coincidence with the FI and BIX indices. It was worth mentioning that the homogeneous nature of OM characteristics between the calcareous soil, paddy soil, and lake sediment, as indicated by similar fluorophores, existed in those extracted HA and FA fractions. This was further supported by the ultraviolet spectra and the molecular weight distributions of HS. In addition, the soil erosion evolution was well documented by the profile change of C/N ratios and $\delta^{13}C$ proxies as well as HS composition in sediment since the construction of the lake. Furthermore, this study contributes to a better comprehension of the terrestrial organic

C sink captured by the karst lake and provides a reference for future studies tracking natural OM compositional changes in response to human disturbance and/or climate change.

Acknowledgments The two anonymous reviewers are particularly appreciated for their valuable comments that greatly improved the manuscript. We also thank Prof. M. G. Mostofa Khan, Tianjin University, China, for the assistance in language editing.

Author contributions RZ: Conceptualization, Resources, Project administration, Supervision, Data curation, Formal analysis, Validation, Visualization, Writing-original draft, Writing-review & editing, Funding acquisition. LW: Methodology, Investigation, Formal analysis, software, Visualization, Writing-original draft. JC: Writing-original draft.

Funding This study was financially supported by the Strategic Priority Research Program of Chinese Academy of Sciences (XDB40020504), and the National Natural Science Foundation of China (U1612442, 41573133, 41867048).

Availability of data and materials The datasets used and/or analyzed during the current study are available from the corresponding author on reasonable request.

Compliance with ethical standards

Competing interests The authors declare that they have no competing interests.

Ethical approval Not applicable.

Consent to participate Not applicable.

Consent to publish Not applicable.

References

Anderson N, Dietz R, Engstrom D (2013) Land-use change, not climate, controls organic carbon burial in lakes. Proc R Soc Lond B Biol Sci 280:20131278

Anderson N, Bennion H, Lotter A (2014) Lake eutrophication and its implications for organic carbon sequestration in Europe. Glob Chang Biol 20:2741–2751

Artinger R, Buckau G, Geyer S, Fritz P, Wolf M, Kim J (2000) Characterization of groundwater humic substances: Influence of sedimentary organic carbon. Appl Geochem 15:97–116

Calace N, Furlani G, Petronio BM (2000) Sedimentary humic and fulvic acids: Structure, molecular weight distribution and complexing capacity. Ann Chim 90:25–34

Chen JA, Zeng Y, Yu J, Wang JF, Yang HQ, Lu YT (2019) Preferential regeneration of P relative to C in a freshwater lake. Chemosphere 222:15–21

Chin YP, Aiken GR, Oloughlin E (1994) Molecular weight, polydispersity, and spectroscopic properties of aquatic humic substances. Environ Sci Technol 28:1853–1858

Coble PG (1996) Characterization of marine and terrestrial DOM in seawater using excitation-emission matrix spectroscopy. Mar Chem 51: 325–346

Cole JJ, Prairie YT, Caraco NF, McDowell WH, Tranvik LJ, Striegl RG, Duarte CM, Kortelainen P, Downing JA, Middelburg JJ, Melack J (2007) Plumbing the global carbon cycle: integrating inland waters into the terrestrial carbon budget. Ecosystems 10:171–184

Derrien MKL, Jae-Eun P, Li P, Chen M, Sang HL, Soo HL, Jun-Bae L, Jin H (2017) Spectroscopic and molecular characterization of humic substances (HS) from soils and sediments in a watershed: comparative study of HS chemical fractions and the origins. Environ Sci Pollut Res 24:16933–16945

Di X, Xiao B, Dong H, Wang S (2019) Implication of different humic acid fractions in soils under karst rocky desertification. Catena 174: 308–315

Einsele G, Yan J, Hinderer M (2001) Atmospheric carbon burial in modern lake basins and its significance for the global carbon budget. Glob Planet Chang 30:167–195

Fang J, Wu F, Xiong Y, Wang S, Yang H (2017) A comparison of the distribution and sources of organic matter in surface sediments collected from northwestern and southwestern plateau lakes in China. J Limnol 76:571–580

Fellman JB, Hood E, Spencer RGM (2010) Fluorescence spectroscopy opens new windows into dissolved organic matter dynamics in freshwater ecosystems: a review. Limnol Oceanogr 55:2452–2462

Fuse Y, Okamoto T, Hayakawa K, Karatani H, Yamada E (2016) Py-GC/MS analysis of sediments from Lake Biwa, Japan: characterization and sources of humic acids. Limnology 17:207–221

Goni MA, Teixeira MJ, Perkey DW (2003) Sources and distribution of organic matter in a river dominated estuary (Winyah Bay, SC, USA). Estuar Coast Shelf S 57:1023–1048

Hayes MHB, Clapp CE (2001) Humic substances: considerations of compositions, aspects of structure, and environmental influences. Soil Sci 166:723–737

He H, Liu Z, Chen C, Wei Y, Bao Q, Sun H, Yan H (2020) The sensitivity of the carbon sink by coupled carbonate weathering to climate and land-use changes: Sediment records of the biological carbon pump effect in Fuxian Lake, Yunnan, China, during the past century. Sci Total Environ 720:137539

Heathcote AJ, Downing JA (2012) Impacts of eutrophication on carbon burial in freshwater lakes in an intensively agricultural landscape. Ecosystems 15:60–70

Huguet A, Vacher L, Relexans S (2009) Properties of fluorescent dissolved organic matter in the Gironde Estuary. Org Geochem 40: 706–719

Hur J, Hang V, Lee BM (2014) Influence of upstream land use on dissolved organic matter and trihalomethane formation potential in watersheds for two different seasons. Environ Sci Pollut Res 21:7489–7500

Hur J, Lee DH, Shin HS (2009) Comparison of the structural, spectroscopic and phenanthrene binding characteristics of humic acids from soils and lake sediments. Org Geochem 40:1091–1099

Jiang YB, Ji HB (2013) Isotopic indicators of source and fate of particulate organic carbon in a karstic watershed on the Yunnan-Guizhou Plateau. Appl Geochem 36:153–167

Jiang ZC, Lian YQ, Qin XQ (2014) Rocky desertification in Southwest China: Impacts, causes, and restoration. Earth Sci Rev 132:1–12

Kendall C, Coplen TB (2001) Distribution of oxygen-18 and deuterium in river waters across the United States. Hydrol Process 15:1363–1393

Lamb AL, Wilson GP, Leng MJ (2006) A review of coastal palaeoclimate and relative sea-level reconstructions using $\delta^{13}C$ and C/N ratios in organic material. Earth Sci Rev 75:29–57

Lechleitner FA, Dittmar T, Baldini JUL, Prufer KM, Eglinton TI (2017) Molecular signatures of dissolved organic matter in a tropical karst system. Org Geochem 113:141–149

Li GR (2009) Cascade damming of the river and its phytoplankton evolution carbon isotope compositions-a case study of Maotiao River drainage area in Guizhou Province. PhD Dissertation, Guizhou Normal Univ., China (in Chinese with English abstract)

Li Z, Xu X, Yu B, Xu C, Liu M, Wang K (2016) Quantifying the impacts of climate and human activities on water and sediment discharge in a karst region of southwest China. J Hydrol 542:836–849

Long S, Hamilton PB, Yang Y, Ma J, Chobet OC (2018) Multi-year succession of cyanobacteria blooms in a highland reservoir with changing nutrient status, Guizhou Province, China. J Limnol 77: 232–246

Lu W, Wang S, Yeager KM, Liu F, Huang Q, Yang Y (2018) Importance of considered organic versus inorganic source of carbon to lakes for calculating net effect on landscape C budgets. J Geophys Res-Biogeo 23:1302–1317

Lü W, Yao X, Shao K, Zhang B, Gao G (2019) Unraveling the sources and fluorescence compositions of dissolved and particulate organic matter (DOM and POM) in Lake Taihu, China. Environ Sci Pollut Res 26:4027–4040

Luo G, Wang S, Bai X, Liu X, Cheng A (2016) Delineating small karst watersheds based on digital elevation model and eco-hydrogeological principles. Solid Earth 7:457–468

Luo Y, Lu M, Wang H, Qiu A (2019) Recent soil erosion in the Hongfeng catchment on the Guizhou Plateau, SW China revealed by analysis of reservoir sediments and soil loss modeling. J Paleolimnol 61:17–35

Ma L, Xiao B, Di X, Huang W, Wang S (2016) Characteristics and distributions of humic acids in two soil profiles of the southwest China Karst area. Acta Geochim 35:85–94

Meyers PA (1994) Preservation of elemental and isotopic source identification of sedimentary organic matter. Chem Geol 114:289–302

Meyers PA, Ishiwatari R (1993) Lacustrine organic geochemistry-an overview of indicators of organic matter sources and diagenesis in lake sediments. Org Geochem 20:867–900

Nguyen HVM, Hur J (2011) Tracing the sources of refractory dissolved organic matter in a large artificial lake using multiple analytical tools. Chemosphere 85:782–789

Nõges P, Fabien C, Alo L, Tõnu M, Eva-Ingrid R, Kaire T, Malle V, Sirje V, Tiina N (2016) Role of a productive lake in carbon sequestration within a calcareous catchment. Sci Total Environ 550:225–230

Perdue EM, Koprivnjak J (2007) Using the C/N ratio to estimate terrigenous inputs of organic matter to aquatic environments. Estuar Coast Shelf S 73:65–72

Peuravuori J, Pihlaja K (1997) Isolation and characterization of natural organic matter from lake water: comparison of isolation with solid adsorption and tangential membrane filtration. Environ Int 23:441–451

Phillips DL (2001) Mixing models in analyses of diet using multiple stable isotopes: A critique. Oecologia 127:166–170

Qianqiu L (2019) Assessing the effects of climate change on water quality of plateau deep-water lake-a study case of Hongfeng Lake. Sci Total Environ 647:1518–1530

Santín C, Yamashita Y, Otero XL, Álvarez MÁ, Jaffé R (2009) Characterizing humic substances from estuarine soils and sediments by excitation-emission matrix spectroscopy and parallel factor analysis. Biogeochemistry 96:131–147

Senesi N, Plaza C, Brunetti G, Polo A (2007) A comparative survey of recent results on humic-like fractions in organic amendents and effects on native soil humic substances. Soil Biol Biochem 39:1244–1262

Sironić A, Jadranka HN, Brozinčević A, Vurnek M, Kapelj S (2017) Changes in the geochemical parameters of karst lakes over the past three decades—the case of Plitvice Lakes, Croatia. Appl Geochem 78:12–22

Sobek S, Tranvik LJ, Prairie YT, Kortelainen P, Cole JJ (2007) Patterns and regulation of dissolved organic carbon: an analysis of 7500 widely distributed lakes. Limnol Oceanogr 52:1208–1219

Sobek SE, Durisch-Kaiser RZ, Wongfun N, Wessels M, Pasche N, Wehrli B (2009) Organic carbon burial efficiency in lake sediments controlled by oxygen exposure time and sediment source. Limnol Oceanogr 54:2243–2254

Song K, Wen Z, Shang Y, Yang H, Lyu L, Liu G, Fang C, Du J, Zhao Y (2018) Quantification of dissolved organic carbon (DOC) storage in lakes and reservoirs of mainland China. J Environ Manag 217:391–402

Stedmon CA, Markager S (2005) Tracing the production and degradation of autochthonous fractions of dissolved organic matter by fluorescence analysis. Limnol Oceanogr 50:1415–1426

Stevenson FJ (1994) Humus chemistry: genesis, composition, reactions. John Wiley and Sons, New York

Swift RS (1996) Organic matter characterization. In: Sparks DL (ed) Methods of soil analysis, Soil Science Society of America Book Series 5. Soil Science Society of America and American Society of Agronomy, Madison, pp 1011–1069

Tranvik LJ, Downing JA, Cotner JB, Loiselle SA, Striegl RG, Ballatore TJ, Dillon P, Finlay K, Fortino K, Knoll LB, Kortelainen PL, Kutser T, Larsen S, Laurion I, Leech DM, McCallister SL, McKnight DM, Melack JM, Overholt E, Porter JA, Prairie Y, Renwick WH, Roland F, Sherman BS, Schindler DW, Sobek S, Tremblay A, Vanni MJ, Verschoor AM, von Wachenfeldt E, Weyhenmeyer GA (2009) Lakes and reservoirs as regulators of carbon cycling and climate. Limnol Oceanogr 54:2298–2314

Traversa A, D'Orazio V, Mezzapesa GN, Bonifacio E, Farrag K, Senesi N, Brunetti G (2014) Chemical and spectroscopic characteristics of humic acids and dissolved organic matter along two Alfisol profiles. Chemosphere 111:184–194

Tremblay L, Gagne J (2009) Organic matter distribution and reactivity in the waters of a large estuarine system. Mar Chem 116:1–12

Trickovic J, Ivancev-Tumbas I, Dalmacija B, Nikolic A, Trifunovic S (2007) Pentachlorobenzene sorption onto sediment organic matter. Org Geochem 38:1757–1769

Wan GJ (1999) ^{137}Cs dating by annual distinguish for recent sedimentation: samples for Erhai and Hongfeng Lake. Quat Sci 1:73–80

Wang HY, Huo YY, Zeng LY, Wu XQ, Cai YL (2008) A 42-yr soil erosion record inferred from mineral magnetism of reservoir sediments in a small carbonate-rock catchment, Guizhou Plateau, southwest China. J Paleolimnol 40:897–921

Wang LY, Wu FC, Zhang RY, Li W, Liao HQ (2009) Characterization of dissolved organic matter fractions from Lake Hongfeng Southwestern China Plateau. J Environ Sci 21:581–588

Wang M, Wu J, Chen H, Yu Z, Zhu Q, Peng C, Anderson NJ, Luan J (2018) Temporal-spatial pattern of organic carbon sequestration by Chinese lakes since 1850. Limnol Oceanogr 63:1283–1297

Wang S, Yeager KM, Wan G, Liu C, Wang Y, Lü Y (2012) Carbon export and HCO_3^- fate in carbonate catchments: a case study in the karst plateau of southwestern China. Appl Geochem 27:64–72

Wang Z, Yin XL, Wan L, Xu CM, Zhang MJ (2019) Dynamics of nitrogen, phosphorus, and organic pollutant losses from a small watershed in the drinking-water source protection area in Guiyang City of Southern China. Environ Sci Pollut Res 26:1791–1808

Wolfe AP, Kaushal SS, Fulton JR, McKnight DM (2002) Spectrofluorescence of sediment humic substances and historical changes of lacustrine organic matter provenance in response to atmospheric nutrient enrichment. Environ Sci Technol 36:3217–3223

Yamashita Y, Jaffé R (2008) characterizing the interactions between trace metals and dissolved organic matter using excitation−emission matrix and parallel factor analysis. Environ Sci Technol 42:7374–7379

Yang Y (2017) Study on DIC/POC concentration, sediments organic carbon and carbon isotope in cascade reservoirs in the middle and upper reaches of Wujiang River. PhD Dissertation, Institute of Geochemistry of the Chinese Academy of Sciences, China (in Chinese with an English abstract)

Zhang J, He M, Lin C, Shi Y (2010) Phenanthrene sorption to humic acids, humin, and black carbon in sediments from typical water systems in China. Environ Monit Assess 166:445–459

Zhang R, Wang L, Chen J (2014a) Physical-chemical characteristics and phosphorus distribution in soils of the Lake Hongfeng watershed in dry seasons. Earth Environ 42:719–725 (in Chinese with English abstract)

Zhang Y, Du J, Zhao X, Wu W, Peng B, Zhang J (2014b) A multi-proxy study of sedimentary humic substances in the salt marsh of the Changjiang. Estuary, China. Estuar Coast Shelf S 151:295–301

Zhou Y, Zhang Y, Shi K, Liu X, Niu C (2015) Dynamics of chromophoric dissolved organic matter influenced by hydrological conditions in a large, shallow, and eutrophic lake in China. Environ Sci Pollut Res 22:12992–13003

Zhu S, Liu C, Tao F, Wang Z, Piao H (2007) Difference in stable carbon isotope composition and profile distribution of soil organic matter between brown limestone soil and yellow soil in karst areas of Guizhou Province. Acta Pedol Sin 44:169–173 (in Chinese with English abstract)